TITLE

DNA delivery to "ex vivo" human liver segments

Authors

María José Herrero[1,2], Luis Sabater[3], Guillermo Guenechea[4], Luis Sendra[1], Ana Isabel Montilla[1], Rafael Abargues[5], Vicente Navarro[6], Salvador F. Aliño[1,2],

Affiliation of authors

[1]Departamento de Farmacología, Facultad de Medicina, Universidad de Valencia, Spain

[2] Unidad de Farmacología Clínica, Servicio de Farmacia, Hospital Universitario La Fe, Valencia, Spain

[3]Servicio de Cirugía, Hospital Clínico Universitario, Valencia, Spain

[4]CIEMAT-CIBERER Hematopoiesis and Gene Therapy Division, Madrid, Spain

[5]Instituto de Ciencia de Materiales. Universidad de Valencia, Spain

[6]Servicio de Radiología. Hospital Universitario La Fe. Valencia, Spain

Correspondence should be addressed to: S.F.A. (alino@uv.es)

This work has been done in Valencia, Spain

Corresponding author´s address:

Departamento de Farmacología

Facultad de Medicina. Universidad de Valencia

Av. Blasco Ibáñez 15

46010 - Valencia (Spain)

Phone: +34-96/3864621; Fax: +34-96/3864972

Running title: Naked DNA delivery to *ex vivo* human liver segments

This work has been partially supported by projects from the *Generalidad Valenciana* (AP-095/09) and the *Ministerio de Ciencia e Innovación* (SAF2007-64492, SAF2011-27002).

Final word count (excluding references and figure text): 5.304

ABSTRACT

Hydrodynamic injection is an efficient procedure for liver gene therapy in rodents but with limited efficacy in large animals, using an "in vivo" adapted regional hydrodynamic gene delivery system. We study the ability of this procedure to mediate gene delivery in human liver segments obtained by surgical resection. Watertight liver segments were retrogradely injected from hepatic vein with a saline solution containing a plasmid bearing the eGFP gene, under different conditions of flow rate (1, 10 and 20 ml/s) and final perfused volume. Samples were cultured 1-2 days and used for microscopy and molecular analysis of gene expression. The fluorescent and immunohistochemistry studies indicated that in segments injected at ≥ 10ml/s, good and wide gene expression is present in the liver sections and the molecular analysis reinforced the histological observation in a quantitative manner (index of apparent gene delivery: 10^2-10^4 eGFP DNA copy/100 pg of total DNA; transcription index: 10^5-$2x10^6$ eGFP RNA copy/100 ng of total RNA). In addition, injected gold nanoparticles (15 nm diameter) suggested that DNA delivery to hepatocytes must involve a facilitated permeation process without membrane disruption. In summary, we show that retrograde venous injection of watertight human liver segment is an anadromous procedure that results in wide liver gene delivery and good gene expression. However, additional studies will be necessary to clarify the influence of the prolonged ischemia injury to hepatocytes in our model.

Key words: Gene delivery, human, liver, catheter, naked DNA, hydrodynamic

INTRODUCTION

The present study has been designed to explore the capacity of regionally hydrodynamic gene delivery to human liver segments, employing an "ex vivo" catheterization procedure. Hydrodynamic gene transfer[1,2] with naked DNA is a safe and efficient method for gene delivery, and we had reported advances in the efficacy of naked DNA gene delivery to mice liver, resulting in long-term therapeutic plasma levels of the protein encoded by the exogenous gene[2]. Since the suggested mechanism underlying the important efficacy of liver gene delivery involves transient inversion of intraorgan blood flow, we had the opportunity to improve the technique and apply it to larger animals, using catheterization procedures – as suggested by preliminary results from both other authors and our own group[3-5]. The gene expression efficiency achieved by this procedure is lower than that achieved by the original mouse procedure involving hydrodynamic tail vein injection[2]. However, the results suggest that liver gene therapy is a promising strategy in which the large liver size and/or the less compliant connective tissue framework of large animals limit the efficiency of liver gene transfer. In this respect there is experimental evidence that promising results are achieved in less elastic cardiac tissue[6], and that outflow obstruction during DNA hepatic vein injection significantly contributes to increase the efficiency of hydrodynamic liver gene delivery[7]. Since all blood vessels are sealed in surgically derived human liver segments, we employ such watertight liver segments to evaluate the efficacy of anadromous naked DNA delivery mediated by hydrodynamic retrovenous injection.

The present study shows that catheter-mediated retrograde injection of naked DNA bearing the eGFP marker gene in the hepatic vein of "ex vivo" human liver segments results in wide anadromous gene delivery and gene expression, without dramatic morphological changes in the liver tissue as evidenced by electron microscopy and the liver distribution of 15 nm gold particles. We must take into consideration that having performed our experiments in liver ischaemic segments of patients undergoing resection due to hepatic cancer, additional experiments are required to confirm the results in a less prolonged ischaemic situation.

RESULTS

Catheterization

The catheter was placed in hepatic vein of the liver segment, and vascular permeation of the liver segment was monitored by fluoroscopy after the injection of contrast solution.

Figure 1 is representative of all the experiments and shows the fluoroscopic position of the catheter with respect to its anatomical location (A and B panels) and the vascular tree after the injection of 5 and 10 ml of contrast solution (C and D panels), respectively. The place where liver samples were taken for molecular analysis can be observed in panel B, corresponding to the right direction of injection, zone A samples, and lateral perfusion areas, zone B samples. We cannot know if contrast solution injection affects eGFP expression since we have injected contrast in all our experiments. For this reason, we always have tried to employ the minimum necessary quantity (volume ≤1% segment weight).

Histological study of eGFP expression

Three different groups were analyzed by fluorescence and/or immunohistochemical procedures. One was injected at 20 ml/s, 1/10 volume of segment weight and gene expression was evaluated by fluorescence microscopy (Fig. 2: A, B, C). The second group was injected at 10 ml/s, 1/5 volume of segment weight and gene expression was evaluated by immunohistochemistry (Fig. 2: E, F, G). The last group was injected at 1 ml/s, 1/5 volume of segment weight and gene expression was evaluated by both fluorescence (Fig. 2D) and immunohistochemistry (Fig. 2H) procedures. Then, small liver samples (1x0.5 cm) measuring < 1 mm in thickness were cultured, and one and two days after gene transfer we studied eGFP gene expression in histological liver sections, employing fluorescent and immunohistochemical procedures. The results show that one day after injection, the fluorescence was clearly observed and widely distributed in liver cryosections from liver segments injected at a 20 ml/s and 1/10 of the segment weight (Fig.2: A-C), thus suggesting that efficient gene delivery was achieved by this procedure. Immunohistochemistry was also employed to detect eGFP expression. In these experiments, injection was performed at 10 ml/s flow rate and with 1/5 segment weight volume. Specific immunostaining one day after injection in paraffin sections from formalin fixed liver samples is observed in Figs. 2F and G, as compared to immunohistochemistry control performed in absence of specific primary antibody (Fig. 2E). In contrast, in livers injected with 1ml/s, volume of 1/5 segment weight, a very limited fluorescence was observed in two of the four liver segments studied. Even in those cases, only two or three microscopic fields of the whole histological section showed a very light fluorescence (Fig. 2D). Moreover, in our hands, the immunohistochemistry staining was negative in all cases (Fig. 2H).

Although the expected reactivity must be lower than with cryosections from frozen samples, a positive reaction was clearly observed in groups injected at 10 ml/s speed or more; however, comparative efficacy determination between the two procedures required molecular analysis.

Quantitative PCR and RT-PCR assays of eGFP

In order to determine the influence of flow rate (20 vs 10 ml/s vs 1ml/s) and total volume (1/10 vs 1/5 segment weight) of the injection upon gene transfer efficacy, we included an additional group (flow rate 20 ml/s and 1/5 ml volume of segment weight) in the above described histochemical study resulting in the following groups: 20 ml/s (1/10 vol), 20 ml/s (1/5 vol), 10 ml/s (1/5 vol), 1 ml/s (1/5 vol) whose pressures during hydrodynamic injection, in the tip of the introducer, were 122.0 ± 102.1, 190.8 ± 79.4, 93.4 ± 33.4 and 25.0 ± 12.3 mm Hg, respectively.

After liver segment transfection, performed as explained in Methods, cultured samples were collected on days 1 and 2 after transfection to evaluate the index of both apparent gene delivery and transcription, on the basis of the number of molecule copies, employing quantitative PCR and RT-PCR, respectively. Several samples were collected from each segment after injection, always belonging to tissue areas corresponding to those seen to be perfused by the contrast pre-injection. The gene expression data obtained were not significantly different between samples A and B from each segment, being A the area directly perfused and B the areas corresponding to lateral zones. The index of apparent eGFP gene delivery to liver tissue was evaluated as the ratio of eGFP DNA copies per 100 pg of total DNA. The term “apparent” tries to remark that the index evaluates the total amount of DNA present in the tissue, without differentiating the functional ability. The results are summarized in Figure 3A, and indicate that the transgene was present in all liver tissue samples but significant differences were observed between groups: maximal values were observed in the 20 ml/s, 1/5 group, being statistically different from all other groups in zone A at the second day ($p < 0,01$). The transcription index was evaluated as the amount of eGFP RNA copies per 100 pg of total RNA. The results are summarized in Figure 3B, and indicate that the transgene was present in all liver tissue samples from segments injected at ≥ 10 ml/s reaching from 10^5 to $2x10^6$ copies per 100 ng total RNA, approximately. In all cases, the highest values were observed on day 2 after transfection, but no statistically significant

differences were observed between groups. However, once again, lower values were observed in segments injected with 1 ml/s, 1/5vol ($p < 0,05$, zone B, day 2).

The apparent intrinsic gene efficacy (iE) indicates the amount of RNA produced per gene copy, and was evaluated as the ratio of RNA/DNA copy of eGFP in each sample. We must note that this parameter, as its name indicates, is "apparent", so the values must be interpreted in the context of the experiment, so the presence of extracellular or non functional plasmids cannot be excluded, but it should be an interesting parameter for the relative comparison between groups. The results are summarized in Figure 4, and show that higher apparent iE, 10^4 approximately, was observed in the liver segments transfected with the injection flow rate of 10 ml/s, 1/5 vol, and continued to show similar values on days 1 and 2 post-transfection, being significantly different ($p < 0,01$) to all the other groups. However, in the segments transfected with 20 ml/s, apparent iE was lower (10^3) and decreased one order of magnitude in samples from zone A, day 2 with respect to day 1, mainly when the highest final volume (1/5 of segment weight) was employed. Since iE is largely dependent on cell viability, we suspect that mild transfection conditions should offer cellular advantages for gene expression, as higher flow and volume values could mediate cell damage resulting in a time-dependent gene iE decrease. When perfusion conditions are too slow (1ml/s), the intrinsic efficacy is dramatically reduced (10^{-1} approx.), suggesting that the functionality of the delivered DNA must be very limited. Regarding A and B zones, significant differences between them were only found in 10 ml/s, 1/5 group ($p < 0,01$).

Transmission electron microscopy

Relevant morphological changes in the liver after hydrodynamic injection, mainly endothelial disruption and massive endocytic vesicles in hepatocytes, have been previously described in mouse and pig[2,4,5,8]. To confirm whether these morphological changes also occur in humans, the liver segments were retrogradely injected at a 20 ml/s flow rate with buffered 2.5% glutaraldehyde solution. Then, tissue samples were collected for transmission electron microscopy. Figure 5 shows a representative image at low magnification of a venous sinusoid and four details (boxes a, b, c and d), at higher magnification, of different areas containing vascular endothelium, Disse space and apical hepatocytes. The main morphological changes observed were: a) dilated sinusoid; b) very small changes, if any, in the sinusoidal endothelium, without signs of

disruption; and c) dilated space of Disse at some sites, without massive endocytic vesicles in the hepatocytes. The morphological changes observed in the liver were smaller than expected, suggesting that anadromous DNA delivery to hepatocytes must involve facilitated permeation, not a membrane disruption process.

In order to reveal the possible existence of membrane disruption not directly observed by transmission electron microscopy, other liver segments were retrogradely injected at a 20 ml/s flow rate with buffered 2.5% glutaraldehyde solution containing gold nanoparticles (15 nm in diameter and 10^{12} particles/ml). Because large amounts of gold nanoparticles are necessary for these experiments, the particles were prepared as described in Methods. The morphological characteristics of the nanoparticles and the diameter distribution are presented in Figure 6. The mean nanoparticle diameter employed in this experiment was 15.5 ± 0.3 nm. The gold nanoparticle distribution in the liver segment is shown in Figure 7, where the central image (at low magnification) shows a dilated sinusoid in which specific boxes, corresponding to sites of the endothelium-Disse space-hepatocyte (a, b, c, d), are amplified with the aim of identifying the location of nanoparticles. In all cases, nanoparticles were observed inside the sinusoid or within the Disse space. In no case were nanoparticles observed inside the hepatocytes, thus suggesting the absence of any hepatocyte membrane disruption, and the implication of a facilitated permeation process in DNA delivery to the liver cells.

DISCUSSION

The present work shows that anadromous gene delivery to "ex vivo" human liver segments, mediated by retrograde injection of naked DNA encoding for the eGFP gene in the hepatic vein, results in efficient gene transfer as indicated by: a) eGFP DNA, RNA identified by quantitative PCR, RT-PCR, and b) eGFP protein identified by fluorescent and immunohistochemistry procedures. In our hands, the best of the studied conditions for transfection was retrograde injection of a saline solution of eGFP plasmid (20 µg/ml) at a flow rate of 10 ml/s and a final volume equivalent to 1/5 of the liver segment weight in grams; and c) the ultrastructural studies employing gold nanoparticles suggest that the mechanism of gene delivery must be mediated by a facilitated permeation process, not by hepatocyte membrane disruption.

Important progress has been made in nonviral gene therapy since the hydrodynamic procedure for mouse liver gene delivery was first described[2,8-10]. However, the systemic

perturbation resulting from hydrodynamic injection remains a serious limitation for clinical application, since it can lead to circulatory collapse and even death. To avoid this adverse effect, we have described a retrograde catheter-mediated gene delivery procedure[5] with the aim of locally reproducing the intrahepatic conditions mediated by tail vein hydrodynamic injection. However, all the studies reported in pigs[4,5,11-14] and in human clinical trials[3] indicate that the efficiency of the procedure remains several orders of magnitude lower than observed in mice. The exact reason for the low gene transfer efficiency of retrograde injection is still unknown, but the low resistance of the sinusoid bed must be a very important factor, since DNA can easily travel across the liver segment after hepatic vein injection, reaching the portal vein and then freely returning to the inferior cava vein through another liver segment[15].

In the present work, we hypothesize that human "ex vivo" liver segments must be excellent candidates for anadromous gene transfer, since the outflow of injected DNA solution from the targeted segment is blocked in the surgical removal process. In all cases, vascular patency before injection was confirmed by contrast injection and Rx fluoroscopy. The injection conditions were similar to those employed in pig experiments for catheter mediated "in vivo" gene transfer, but with the advantage of blocking outflow of injected DNA solution. The results indicate that both 20 and 10 ml/s injection flow rates of a plasmid saline solution (20 μg/ml) containing the eGFP gene mediate efficient gene transfer, as observed by light microscopy employing direct fluorescence or immunohistochemistry procedures. This observation confirms the preliminary hypothesis and supports the idea that outflow obstruction during DNA hepatic vein injection significantly contributes to increase the efficiency of hydrodynamic liver gene delivery[7]. However, when segments were injected with high volumes (1/5 vol) but low flow (1ml/s) we hardly find the protein expression in histological sections. The microscopic observations support the good efficacy of gene delivery in groups injected with ≥ 10ml/s, but the eGFP gene encodes for a non-secreted protein that accumulates within the cytoplasm, and therefore the amount of protein is poorly correlated to expression efficacy.

In order to evaluate how delivery and transcription of the eGFP gene contribute to liver gene transfer efficacy, two tissue indexes were used based on the number of DNA or RNA copies. The eGFP gene apparent delivery index (DNA copy number per 100 pg of total DNA) was 10^2 to 10^4 eGFP copies per 100 pg of total DNA, approximately. The liver segments injected with 1 ml/s also showed lower index values. Interestingly, the

value of the index decreases as the injection conditions become milder (in general, 20 ml/s 1/5> 20 ml/s 1/10> 10 ml/s 1/5> 1 ml/s 1/5). However, we must remark that this index is of apparent distribution, and so it does not analyze the functionality of the quantified DNA. Given that the copy number reached by the milder conditions is 10^2, we could think that a great part of the injected DNA could reach the tissue but without functional ability, as supported by histochemical studies summarized in Fig. 2. If we consider that 3,3 pg DNA is equivalent to a haploid human genome[16], our results suggest an equivalent efficacy of 10-1000 eGFP gene copies/cell, approximately.

The eGFP gene transcription index (RNA copy number per 100 ng of total RNA) was 10^5 to $2x10^6$ copies per 100 ng total RNA, approximately, in groups injected with ≥ 10ml/s, but 2-3 orders of magnitude lower when injected with 1 ml/s, 1/5 vol. In all cases, the highest values were observed two days after transfection in groups injected at ≥10 ml/s. Although no significant difference was observed between those groups, the liver segments injected with 10 ml/s showed slightly higher index values at day one post injection.

The apparent gene intrinsic efficacy (iE) (RNA/DNA copy number of a gene) is an interesting parameter, because it indicates gene cell functionality on the base of the efficacy of gene delivery and transcription in the tissue sample. We must note that this "apparent" parameter must be interpreted in the context of the experiment. The presence of extracellular or non functional plasmids cannot be excluded, therefore in those cases in which the proportion of extracellular plasmids was very elevated, the indexes could not be accurate measures of the efficiency. Anyway, they could be interesting parameters for the relative comparison between groups. Our results indicate that apparent iE decreased 10 times from day 1 to 2 after transfection in both groups of liver segments injected at a 20 ml/s flow rate, mainly in A zones where the hydrodynamic impact is higher. However, similar values on the two days were observed in the group injected at a 10 ml/s flow rate. In addition, higher values of apparent iE were also observed in the group of 10 ml/s compared to the groups of 20 ml/s, suggesting that milder injection conditions must offer cell advantages for gene expression, and confirming that outflow obstruction[7] must contribute to increase the efficiency of hydrodynamic liver gene delivery. Interestingly, when the lowest flow was employed (1ml/s), the apparent iE was dramatically reduced up to 5 orders of magnitude, suggesting that in these conditions the efficiency of the hydrodynamic procedure is very low. This finding supports our previous statement that the amount of gene delivered was

292 in great part not able to be functional. We hypothesize, based on these results that, all
293 the procedures of DNA injection with ≥ 10 ml/s mediate a similar efficacy of
294 transcription, as index of transcription shows, and that the special watertight conditions
295 must probably be contributing to reduce the minimum necessary requirements to reach
296 the hydrodynamic gene transfer. However, the more extreme conditions (more speed
297 and volume) contribute to an increase of DNA copies in the tissue (index of apparent
298 gene delivery) but whose functionality (ability of expressing the gene) must probably be
299 limited, since the apparent intrinsic efficacy is lower regarding the milder conditions
300 group (10ml/s). In any case, the mechanism of anadromous gene transfer mediated by
301 hydrodynamic injection remains unclear.
302 Previously, our group (employing simultaneous portal and cava vein pressures and
303 intravital microscopic evaluation of sinusoidal blood circulation) described that the
304 mechanism of hydrodynamic liver gene transfer involves the inversion of sinusoidal
305 blood flow due to transient inversion of portal versus cava vein differential pressures.
306 Also, morphological changes were associated to the intrahepatic pressures, mainly an
307 increased diameter of the sinusoids and Disse space, as well as increased endothelial
308 disruption and the presence of abundant endocytic vesicles in the apical pole of
309 hepatocytes[8]. The rapid increase in both the inferior cava and portal vein pressures
310 mediated by hydrodynamic injection suggests a low vascular resistance, but pressure in
311 the inferior cava vein remains higher for fewer minutes, resulting in an inverted
312 sinusoidal flow. More recently, it has been proposed[17] that during hydrodynamic
313 injection, retrograde DNA solution reaches the portal vein, where the vascular
314 resistance of the intestinal, splenic and pancreatic capillary beds provides efficient
315 outflow obstruction from the portal vein, and thus outflow obstruction is a necessary
316 condition for effective hydrodynamic gene delivery to individual liver segments or
317 lobes[7,18]. The results of the present paper confirm in human "ex vivo" liver segments
318 that outflow obstruction in hydrodynamic injection of the eGFP gene results in wide
319 gene delivery and efficient gene expression.
320 The exact mechanism of gene delivery mediated by hydrodynamic injection remains
321 unknown, but two routes of entry of DNA plasmids into hepatocytes have been
322 suggested: plasma membrane rupture[19] and increased membrane permeation[5,8,20,21],
323 possibly through endocytic vesicles. In the present study we confirm that hydrodynamic
324 injection mediates an increase in sinusoid diameter, with an endothelium that combines
325 both continuous and discontinuous zones, though in no case was generalized disruption

observed. In addition, the usually narrow Disse space presented an expanded aspect compatible with an increased flow/pressure in this territory. Although some endocytic vesicles or at least incipient vesicles were observed in the apical membrane of hepatocytes, we failed to find territories with abundant endocytic processes lining the hepatocyte membrane, as previously described in mouse and pig. We do not know the reason for this difference, and although it could be due to species-related structural differences, the "ex vivo" conditions also imply that liver segments were deprived of vascular supply 2-3 hours before hydrodynamic injection, and therefore a loss of cell endocytic response could be possible. However, we cannot exclude that these discrepancies could be due to suboptimal conditions of the experimental model that could be improved. Although the degree of endocytic vesicles could limit the efficiency of the process, this fact could be compensated by an increase of membrane permeation due to the special conditions of the hepatic segments in our experiments.

To evaluate how this circumstance could contribute to minimal rupture of the plasma cell membrane of hepatocytes permitting DNA entry into the cell, additional experiments were performed, injecting gold nanoparticles with a mean diameter of 15 nm. The results indicate that the nanoparticles were always located in the vascular bed and within the Disse space, but never inside hepatocytes - thus supporting the idea that a permeation process must be involved in the gene transfer process. In this context, facilitated permeation is related to the ability of DNA to cross the cell membrane in the particular scenario of hydrodynamic injection. Two questions must be remarked. Although nanoparticles and plasmid size could be similar, the rigidity characteristics are very different and this could explain their different ability to cross the cell membranes. The second point is that higher concentrations of injected nanoparticles could contribute to clarify the degree of membrane permeation to these particles.

In summary, we have shown that the retrograde venous injection of "ex vivo" human liver segments is an anadromous procedure that can mediate good efficacy of gene delivery and gene expression in human liver, with potential clinical applications. In this respect, we believe that this gene transfer procedure could be a promising option in the field of human liver transplantation, since genetically modified grafts could contribute to decrease ischemia-reperfusion injury or prevent allograft rejection, as recently suggested[22].

MATERIAL AND METHODS

Liver segments

Human liver segments were obtained from surgical resections of tumor metastatic patients. The liver segments come from surgery to patients and the fragments resected are sealed as well as the remaining piece of liver inside the patient, in the manner the surgeons usually do in the clinical practice: the liver parenchyma was sealed by 3/0 silk sutures or staples when the vessels were bigger than 2-3 mm and by electrocautery when smaller.

The number of segments used in the eGFP molecular studies were 19, corresponding to 19 human livers. 14 Samples of 10 of those segments were used for fluorescence or immunohistochemistry. Finally, for ultrastructural changes studies without (n=3) or with gold nanoparticles (n=3), 6 additional human liver segments were employed. Table 1 shows the main characteristics of all the human liver segments (HL) employed, including anatomical situation, segment weight, the experimental injection conditions performed and the kind of analyses in each segment, being PCR, molecular analyses of PCR and/or RT-PCR; F, optical fluorescence microscopy for eGFP protein; IHC, optical microscopy for immunohistochemistry of eGFP protein; TEM, transmission electron microscopy; TEM-Gold, transmission electron microscopy after gold nanoparticles injection.

We state that the Declaration of Helsinki protocols were followed and that patients gave their written, informed consent. This research was approved by the Clinical Research Ethics Committee of the Hospital Clínico Universitario of Valencia (Spain).

Reagents

The primary anti-GFP antibody was obtained from Abcam (ab290, Cambridge, USA), and the peroxidase-conjugated antibody and immunohistochemical developing system (LSAB) were obtained from DAKO (Barcelona, Spain).

The plasmid p3C-EGFP (6.45 Kb), containing the enhanced green fluorescent protein cDNA driven by the pCMV promoter, was constructed by cloning EGFP into the HindIII site of pcDNA3 (Invitrogen, Barcelona, Spain), excised from pEGFP-N1 (4.7 kb) plasmid vector (Clontech Laboratories, Saint-Germain-en-Laye, France).

Gold nanoparticle synthesis

All chemicals were purchased from Sigma-Aldrich (Madrid, Spain) and used as received without further purification. Gold nanoparticles were synthesized following a modification of the Turkevich method[23]. Typically, 0.4 g of HAuCl4.3H2O were dissolved in 90 ml of water in a two-neck round flask (1.3 mM HAuCl4). The resulting solution was heated to boiling and refluxed. Then, 9 ml of a 47.2 mM sodium citrate solution (0.125 g sodium citrate in 9 ml water) was preheated and quickly added. The solution turned from yellow to black and to deep red. After the color changed, the solution was refluxed for 20 minutes. Then, the heater was turned off and the solution was stirred until it reached room temperature. The resulting solution was diluted with water to a final volume of 500 ml. Gold nanoparticles were characterized by transmission electron microscopy (TEM, Jeol 1010, Tokyo, Japan). The average diameter and the size distribution of the gold nanoparticles were determined from TEM images by counting at least 300 nanoparticles using Image Pro Plus software from Media Cybernetics (Bethesda, USA).

"Ex vivo" gene transfer to liver segment

Human liver segments (418.0±227.2 g) were obtained from patients after surgical resection of liver metastases. Samples were immediately transported under humid and sterile box conditions to the laboratory, and all experimental processing was completed in approximately 1.5 hours, employing sterile solutions and aseptic conditions. A flexible 8F introducer (used as catheter), filled with saline solution, was placed into the hepatic vein previously marked by the surgeon. After catheter fixation using needle and thread, in all experiments, contrast solution was injected before hydrodynamic injection to confirm a correct positioning of the catheter and balloon closure of the vein. Always, the contrast injection was at low speed (not hydrodynamical) and employing a maximum volume of approximately 1% of segment weight (3-10ml). The visualization of a well defined vascular tree was required before performing the hydrodynamic injection.

For gene transfer study, a volume of 1/5 or 1/10 of the segment weight, bearing 20 µg/ml of plasmid in saline solution containing the green fluorescent protein gene (eGFP) was injected at a 10 or 20 ml/s flow rate. A low injection flow group was also included being injected at 1 ml/s and with the highest volume, 1/5. During the experiment of hydrodynamic injection, the pressure (mm Hg) at the tip of the introducer was continuously monitorized by means of an auxiliary access. A Spectramed Statham

pressure transducer (model P23XL) and a Grass model 7 polygraph (preamplifier model 7P1J and amplifier model 7DAG) were employed. After injection, we wait five minutes to remove the catheter.

Then, tissue samples were obtained from perfused areas. Tissue samples < 1 mm in thickness were subsequently collected under sterile conditions and cultured in DMEM medium and a 5% CO_2 atmosphere. Samples were removed 1 and 2 days after transfection and processed for molecular analysis to evaluate the efficiency of gene delivery and the persistence of eGFP expression.

For morphological studies, the same procedure was performed, but injecting a solution containing 15 nm gold nanoparticles ($1.8x10^{12}$ Au particles/ml) for further electron microscopy observations.

Quantitative PCR and RT-PCR

Liver tissue samples were cut into small pieces and homogenized in Tri Reagent (Ambion, Applied Biosystems, Madrid, Spain) with an Ultra-Turrax (Hielscher Ultrasonics GmbH, Teltow, Germany) homogenizer. Subsequently, the RNA samples were treated with RNase free DNase (Gibco, Invitrogen, Barcelona, Spain). Further purification with the RNeasy mini-kit (Qiagen, Barcelona, Spain) was performed before spectrophotometric quantification. Retrotranscription to cDNA was performed using 1 µg total RNA (DNA free), Random Hexamers and a High Capacity cDNA Archive kit (Applied Biosystems, Madrid, Spain). For qRT-PCR, power SYBR green PCR master mix (Applied Biosystems, Madrid, Spain) was employed according to the instructions of the manufacturer.

The oligonucleotides were designed with Primer Express software (Applied Biosystems, Madrid, Spain). The primers specific for eGFP were:

FW: 5'-GTA AAC GGC CAC AAG TTC AGC-3', Tm: 53.9 ºC

RV: 5'-TGG TGC AGA TGA ACT TCA GGG-3', Tm: 54.9 ºC

Probe: 5'-6FAM-CTTGCCGTAGGTGGC-MGBNFQ-3'

The precise amount of RNA (based on optical density) and its quality (lack of degradation) were normalized with respect to an endogenous control gene (GAPDH). The quantitative data were calculated as the number of DNA or RNA copies on a regression curve employing the plasmid containing the eGFP gene or full human DNA, considering that 3 pg of DNA contains a genome copy[16].

Statistically significant differences between groups were evaluated by two-way analysis of variance (ANOVA) followed by Bonferroni post-tests, employing Graph Pad Prism 4.02 Software (GraphPad Software, San Diego, California, USA).

Fluorescent and immunohistochemical eGFP identification

For fluorescent study, liver cryosections from human segments (n=7) cultured 24 h after transfection were used. The cryosections were examined and photographed using a Zeiss Axiovert 135 inverted microscope (Carl Zeiss, Madrid, Spain).

For immunohistochemical study, liver samples (n=7) were fixed in 4% paraformaldehyde and embedded in paraffin. Immunostaining was carried out as previously described[2]. Briefly, deparaffinized tissue sections were incubated with 4% bovine serum albumin in PBS (1 hour, 37ºC). Then, the tissue sections were incubated in antibody solution (1:300 diluted rabbit anti-GFP) at 37ºC for one hour. The respective control samples incubated in the absence of specific antibody were included. Detection was carried out using the LSAB-2 peroxidase kit (Dako, Barcelona, Spain). Tissue was counterstained with hematoxylin before dehydration.

Electron microscopy

Human liver segments (n=3) were retrodynamically injected (volume 1/5 of segment weight) through the catheter placed in the hepatic vein with a buffered solution of 2.5% glutaraldehyde. Additional experiments (n=3) were performed under identical conditions of glutaraldehyde injection but containing 10^{12} gold particles/ml, to study the liver distribution of 15 nm gold nanoparticles after injection. Then, in both cases small tissue pieces from different liver areas were removed and immersed in phosphate Sørensen buffer (pH 7.4) solution containing 2.5% glutaraldehyde. For transmission electron microscopy, multiple 1-mm^3 pieces of liver were routinely processed and embedded in Epoxy resin. Ultrathin sections, stained with uranyl acetate and lead citrate, were examined under a Jeol JEM-1010 electron microscope.

ACKNOWLEDGMENTS

The authors thank Mr. Alejo Sempere from the Department of Pathology, University of Valencia, for the immunohistochemistry, the SCSIE from the University of Valencia for the electron microscopy and A. Gonzalez and M.L. Lozano from CIEMAT/CIBERER for qPCR analysis. The manuscript contains no conflicts of interest, no material of

publication which would violate any copyright or other personal or proprietary right of any person or entity. This work has been partially supported by projects from the *Generalidad Valenciana* (AP-095/09) and the *Ministerio de Ciencia e Innovación* (SAF2007-64492 and SAF2011-27002).

499 REFERENCES

500 1. Liu F, Song YK, Liu D. Hydrodynamics-based transfection in animals by systemic
501 administration of plasmid DNA. *Gene Ther* 1999; **6**: 1258-1266
502 2. Aliño SF, Crespo A, Dasí F. Long-term therapeutic levels of human alpha-1-
503 antitrypsin in plasma after hydrodynamic injection of nonviral DNA. *Gene Ther* 2003;
504 **10**: 1672-1679
505 3. Khorsandi SE, Bachellier P, Weber JC, Greget M, Jaeck D, Zacharoulis D, *et al*..
506 Minimally invasive and selective hydrodynamic gene therapy of liver segments in the
507 pig and human. *Cancer Gene Ther* 2008; **15:** 225-30.
508 4. Herrero MJ, Dasi F, Noguera I, Sanchez M., Moret I., Sanmartin I, *et al*. Mouse and
509 pig nonviral liver gene therapy: success and trials. *Gene Ther Mol Biol* 2005; **9**: 169–
510 180.
511 5. Aliño SF, Herrero MJ, Noguera I, Dasi F, Sanchez M. Pig liver gene therapy by
512 noninvasive interventionis catheterism. *Gene Ther* 2007; **14**: 334-343
513 6. Aliño SF, Herrero MJ, Bodi V, Noguera I, Mainar L, Dasi F, *et al*. Naked DNA
514 delivery to whole pig cardiac tissue by coronary sinus retrograde injection employing
515 non-invasive catheterization. *J Gene Med* 2010; **12**: 920-926
516 7. Sawyer GJ, Zhang X, Fabre JW. Technical requirements for effective regional
517 hydrodynamic gene delivery to the left lateral lobe of the rat liver. *Gene Ther* 2010*;* **17**:
518 560-564
519 8. Crespo A, Peydro A, Dasi F, Benet M, Calvete JJ, Revert F, *et al*. Hydrodynamic
520 liver gene transfer mechanism involves transient sinusoidal blood stasis and massive
521 endocytic vesicles, *Gene Ther* 2005; **12**: 927-935
522 9. McTiernan CF, Mathier MA, Zhu X, Xiao X, Klein E, Swan CH, *et al*. Myocarditis
523 following adeno-associated viral gene expression of human soluble TNF receptor
524 (TNFRII-Fc) in baboon hearts, *GeneTher* 2007; **14**: 1613–1622
525 10. Zhang G, Budker V, Wolf JA. High levels of foreign gene expression in hepatocytes
526 after tail vein injections of naked plasmid DNA. *Hum Gene Ther* 1999; 10: 1735-1737
527 11. Hoshino K, Kimura T, De Grand AM, Yoneyama R, Kawase Y, Houser S, *et al*.
528 Three catheter-based strategies for cardiac delivery of therapeutic gelatin microspheres.
529 *Gene Therapy* 2006; **13**: 1320-1327
530 12. Suda T, Suda K, Liu D. Computer-assisted hydrodynamic gene delivery. *Mol Ther*
531 2008*;* **16**: 1098-1104

13. Fabre JW, Grehan A, Whiterhorne M, Sawyer GJ, Dong X, Salehi S, *et al*. Hydrodynamic gene delivery to the pig liver via an isolated segment of the inferior vena cava. *Gene Ther* 2008*;* **15**: 452-462

14. Kamimura K, Suda T, Xu W, Zhang G, Liu D. Image-guide, lobe-sapecific hydrodynamic gene delivery to swine liver. *Mol Ther* 2009*;* **17**: 491-499

15. Eastman SJ, Baskin KM, Hodges BL, Chu Q, Gates A, Dreusicke R, *et al*. Development of catheter-based procedures for transducing the isolated rabbit liver with plasmid DNA. *Hum Gene Ther* 2002; **13**: 2065-2077.

16. Gregory, TR. Animal Genome Size Database (2010). http://www.genomesize.com (accesed on April 2010)

17. Sawyer GJ, Rela M, Davenport M, Whitehorne M, Zhang X, Fabre JW. Hydrodynamic gene delivery to the liver: theoretical and practical issues for clinical application. *Curr Gene Ther* 2009; **9**: 128-135.

18. Fabre JW, Whitehorne M, Grehan A, Sawyer GF, Zhang X, Davenport M, *et al*. Critical physiological and surgical considerations for hydrodynamic pressurisation of individual segments of the pig liver. *Human Gene Ther* 2010; e-pub ahead of print doi:10.1089/hum.2010.144

19. Zhang G, Gao X, Song YK, Volimer R, Stolz DB, Gasiorowski JZ, *et al*. Hydroporation as the mechanism of hydrodynamic delivery. *Gene Ther* 2004; **11**: 675-682.

20. Sebestyén MG, Budker VG, Budker T, Subbotin VM, Zhang G, Monahan SD, *et al*. Mechanism of plasmid delivery by hydrodynamic tail vein injection. I.Hepatocyte uptake of various molecules. *J Gene Med* 2006; **8**: 852-873

21. Suda T, Gao X, Stolz DB, Liu D. Structural impact of hydrodynamic injection on mouse liver. *Gene Ther* 2007; **14**: 129-137.

22. Si ZZ, Li JQ, Ai HA, He ZJ, Hu W, Li YN. Recombinant adenovirus vector Ad-hIL-10 protects grafts from cold ischemina-reperfusion injury following orthotopic liver transplantation in rats. *Heptobiliar Pacreatic Dis Int* 2010*;* **9**: 144.148

23. Kimling J, Maier M, Okenve B, Kotaidis V, Ballot H, Plech A. Turkevic method for gold nanoparticle synthesis revisited. *J Phys Chem* 2006; **110**: 157-60

FIGURE LEGENDS

Figure 1- Catheter position in liver segment

Representative image of Rx fluoroscopy of the catheter placed inside hepatic vein of a liver segment (A) corresponding to VII and VIII human hepatic liver segments, weighting 450g, as compared with the anatomical image of the same liver segment (B), where the cuts represent the places were samples were removed for morphological and molecular analysis, after hydrodynamic injection, being A zone the cut in the middle of the segment corresponding to direct site of injection, and B zone those upper and lower cut corresponding to lateral zones. The small black bars in A panel are the staples used by the surgeon to close the vessels when surgery was performed. C and D panels show the Rx image at the same segment during injection of contrast solution at low speed (<1ml/s, not hydrodynamical) with total volume of 5ml. C panel shows the picture taken with half of the volume injected and D panel, the picture taken at the end of injection.

Figure 2- Fluorescence and immunohistochemistry of eGFP

The fluorescence and immunohistochemistry findings of eGFP in histological liver sections are shown. In the first case (Fig. 2A-C), a saline solution containing the plasmid DNA was injected to liver segment at a 20 ml/s flow rate, with a final volume of 1/10 segment weight. The liver samples were cultured 24 h, then frozen, and the cryosections were used for fluorescent microscopy. The figure shows representative images under x20 magnification. In the second case (Fig. 2E-G), the liver segment was injected at a 10 ml/s flow rate, with a final volume of 1/5 segment weight. After 24 h of culture, eGFP protein was developed by immunohistochemistry in paraffin sections from formalin-fixed tissue. E: image from control immunohistochemical tissue section, developed in the absence of specific primary antibody. F and G: specific immunohistochemical reaction against eGFP protein under x40 magnification. Detection was carried out using the LSAB-2 peroxidase kit. Tissue was counterstained with hematoxylin. Images D and H show the respective experiments of fluorescence and immunohistochemistry from liver segments injected at 1 ml/s flow rate and with 1/5 segment weight volume.

Figure 3- Index of Apparent Gene Delivery and Index of Tissue Transcription

The human liver segments were retrogradely injected with saline solution containing 20 μg/ml of DNA plasmid bearing the eGFP gene. Different groups were established according to the different conditions of flow rate (1, 10 or 20 ml/s) and total volume injected (1/5 or 1/10 of segment weight, g). Quantitative eGFP PCR or RT-PCR was performed in liver tissue samples collected 1 and 2 days after gene transfer from zones A and B, and the eGFP copy number in each sample was calculated on a standard curve using the same transfection plasmid. The index of apparent eGFP gene delivery to liver tissue (Fig. 3A) was calculated as the ratio of eGFP DNA copies per 100 pg of total DNA. Statistical significance by two-way ANOVA analysis and Bonferroni post-test was found in groups marked with * ($p < 0,01$) compared to 20 ml/s, 1/5 group. The index of tissue transcription (Fig. 3B) was calculated as the number of eGFP RNA copies per 100 pg of total RNA. No statistically significant differences were observed between groups except for 1 ml/s, 1/5 ($p < 0,05$) by two-way ANOVA and Bonferroni post-test, marked with *.

Figure 4- Index of Apparent Gene Intrinsic Efficacy in Liver Tissue

Experimental conditions of transfection and molecular analysis of the liver samples were as described in Figure 3. The index of apparent intrinsic gene efficacy (iE) was calculated as the ratio of RNA/DNA copy of eGFP in each sample, and indicates the amount of RNA produced per DNA gene copy. The statistical significance between groups is indicated as * ($p < 0,01$) when comparing groups against 10 ml/s, 1/5. The symbol # ($p < 0,01$) indicates statistical significance between A and B zones inside the group by two-way ANOVA and Bonferroni post-test.

Figure 5- Ultrastructural morphological changes

The liver segment was retrogradely injected at a 20 ml/s flow rate with a buffered 2.5% glutaraldehyde solution, and tissue samples were taken for transmission electron microscopy. In the middle, a vessel surrounded by hepatocytes is shown at low magnification (bar = 10 μm), and squares indicate the respective areas at higher magnification for identifying morphological changes in vascular endothelium, Disse space and apical hepatocyte membrane. Arrows: discontinuous endothelium; Star: endocytic vesicles or incipient vesicles; White arrow: Disse space; Bar of square b: 500 nm; Bars of squares a, c and d: 1000 nm).

Figure 6- Gold nanoparticle characterization

The gold nanoparticles were prepared as described in Methods. The morphological characteristics of the gold nanoparticles were examined by transmission electron microscopy (6B), and the average diameter and size distribution (6A) were determined by counting at least 300 nanoparticles.

Figure 7- Gold nanoparticle distribution in the liver segment

The liver segment was retrogradely injected at a 20 ml/s flow rate with buffered 2.5% glutaraldehyde solution plus gold nanoparticles (15 nm in diameter and 10^{12} particles/ml). The central image (at low magnification) shows a dilated sinusoid where specific boxes corresponding to sites of the endothelium-Disse space-hepatocyte (a, b, c, d) are amplified and then again enlarged (a1-a3, b1, c1-c2 and d1) with the aim of identifying the location of nanoparticles. The latter are observed within the sinusoids and the Disse space, but not inside the hepatocytes.

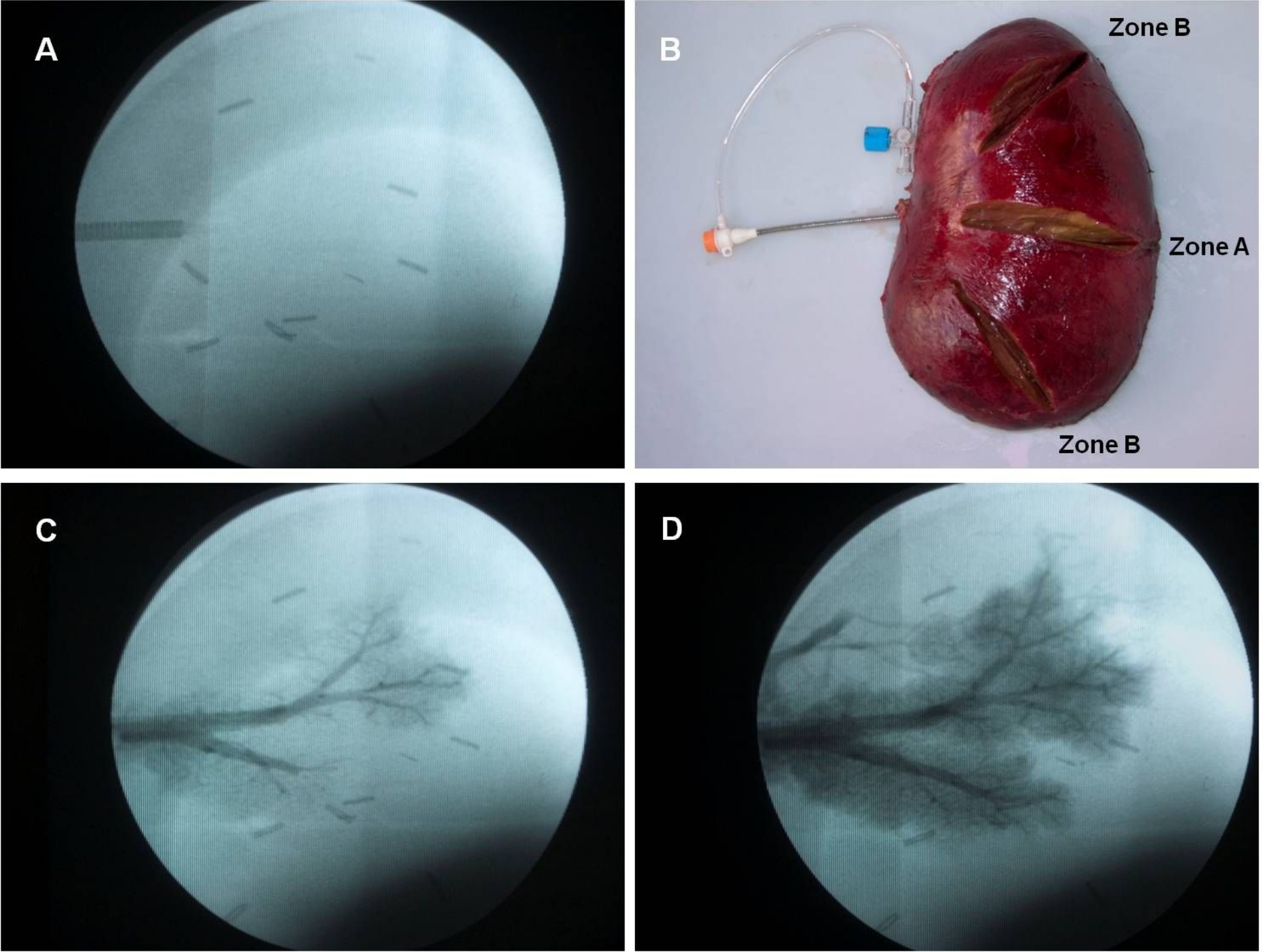
A
B
Zone B
Zone A
Zone B
C
D

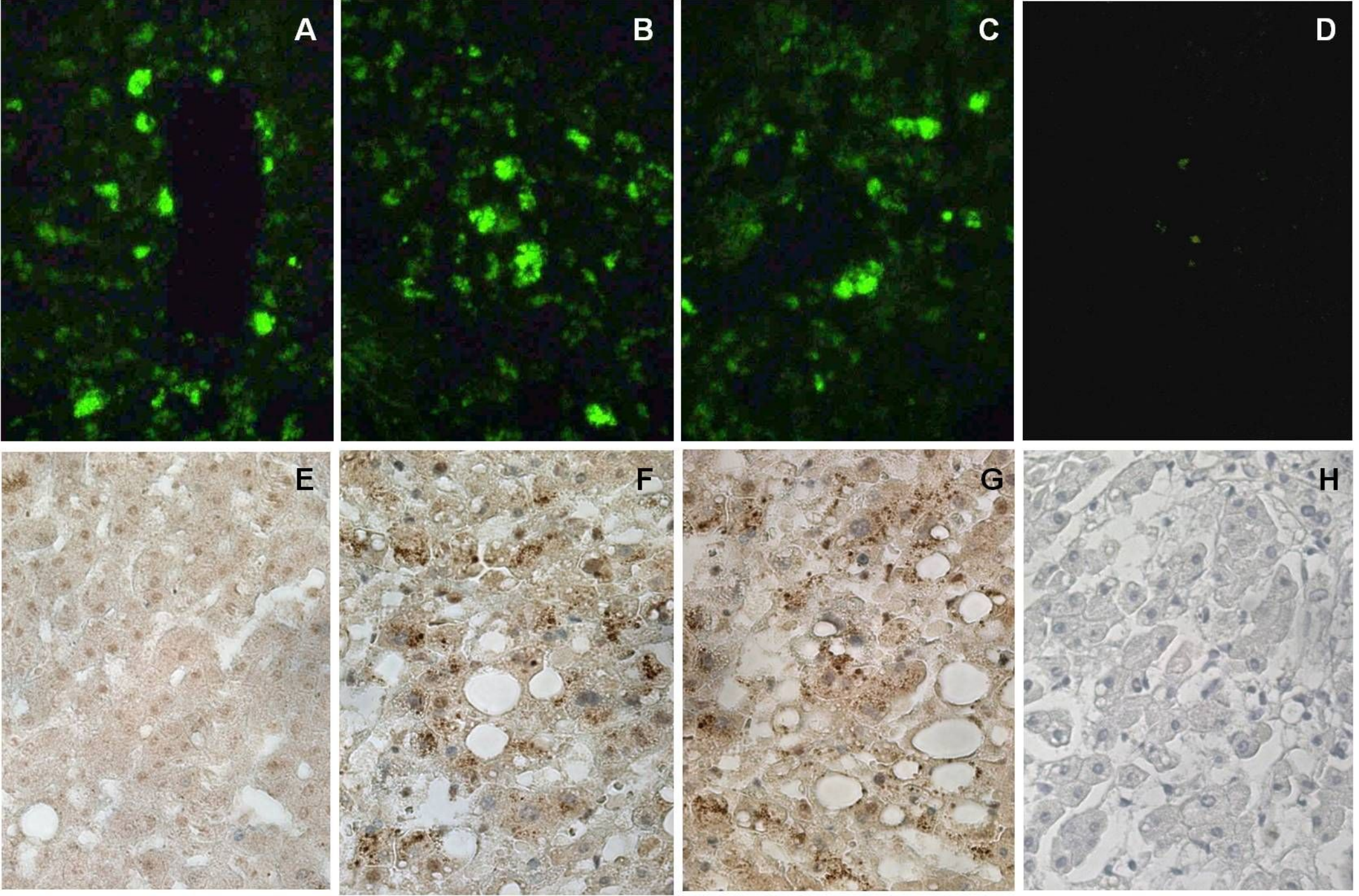
A
B
C
D
E
F
G
H

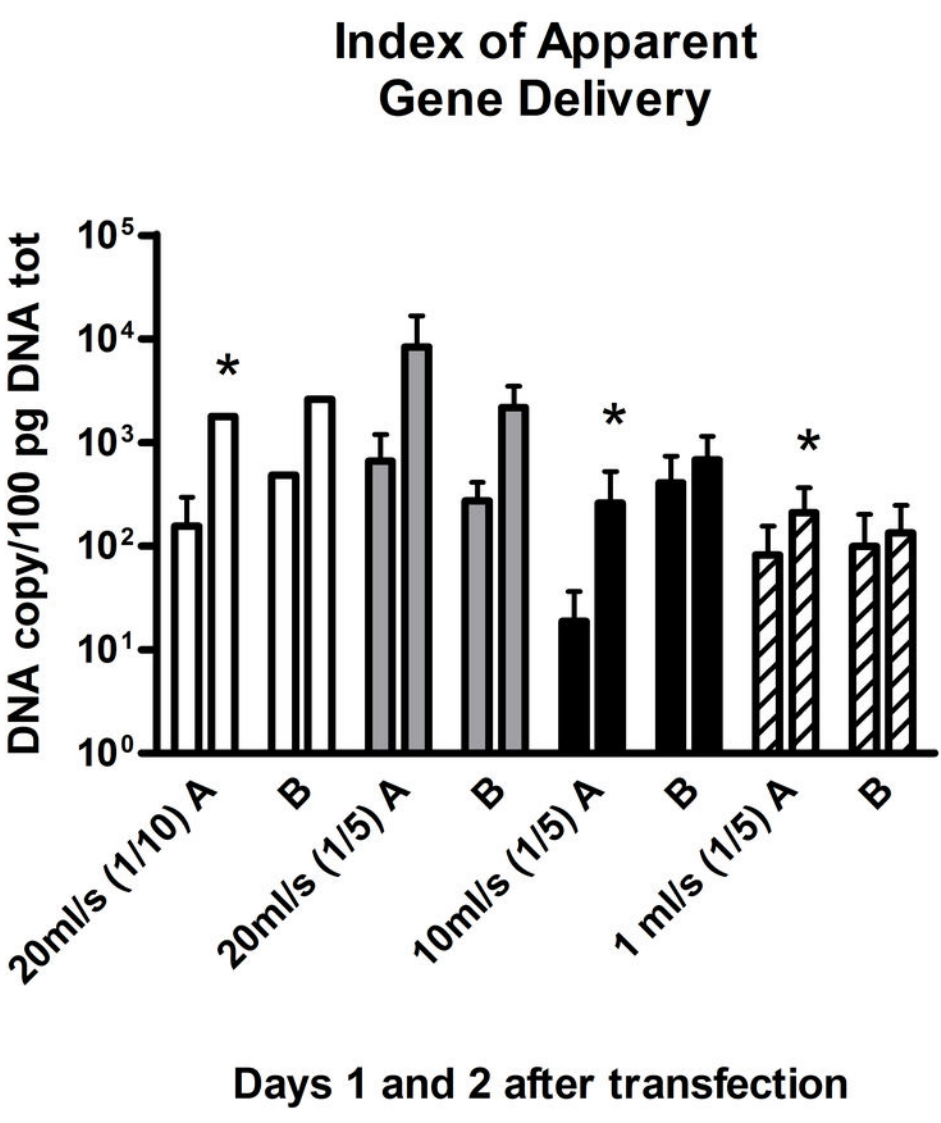
Index of Apparent
Gene Delivery
DNA copy/100 pg DNA tot
10^5
10^4
10^3
10^2
10^1
10^0
*
*
*
20ml/s (1/10) A
B
20ml/s (1/5) A
B
10ml/s (1/5) A
B
1 ml/s (1/5) A
B
Days 1 and 2 after transfection

Index of Tissue Transcription

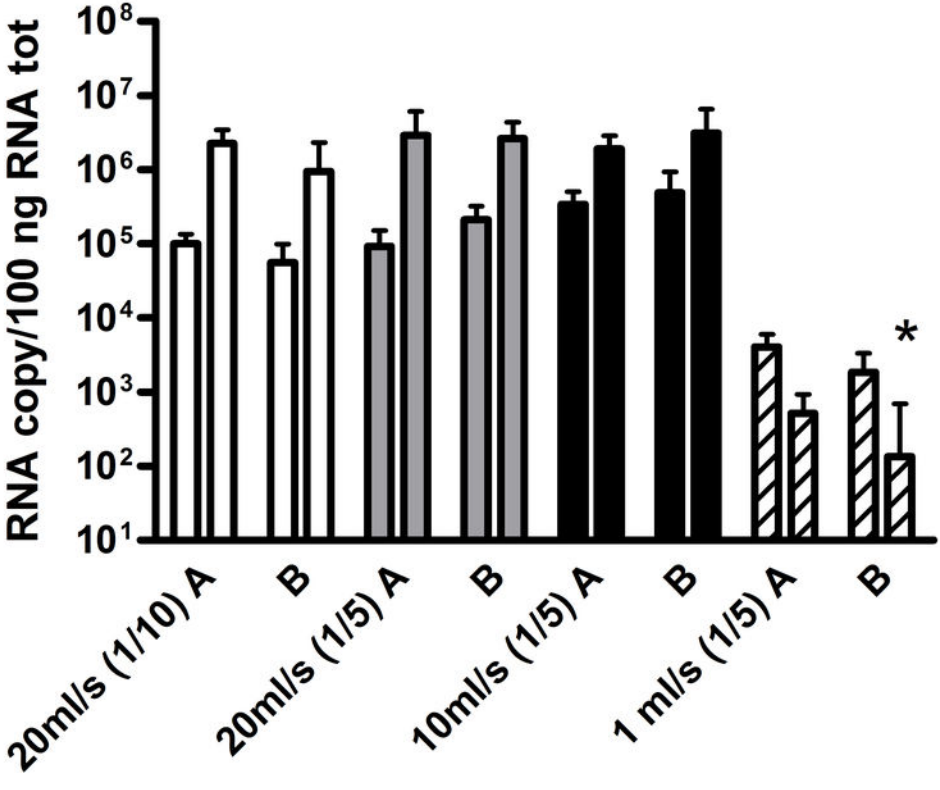

Index of Apparent Gene Intrinsic Efficacy

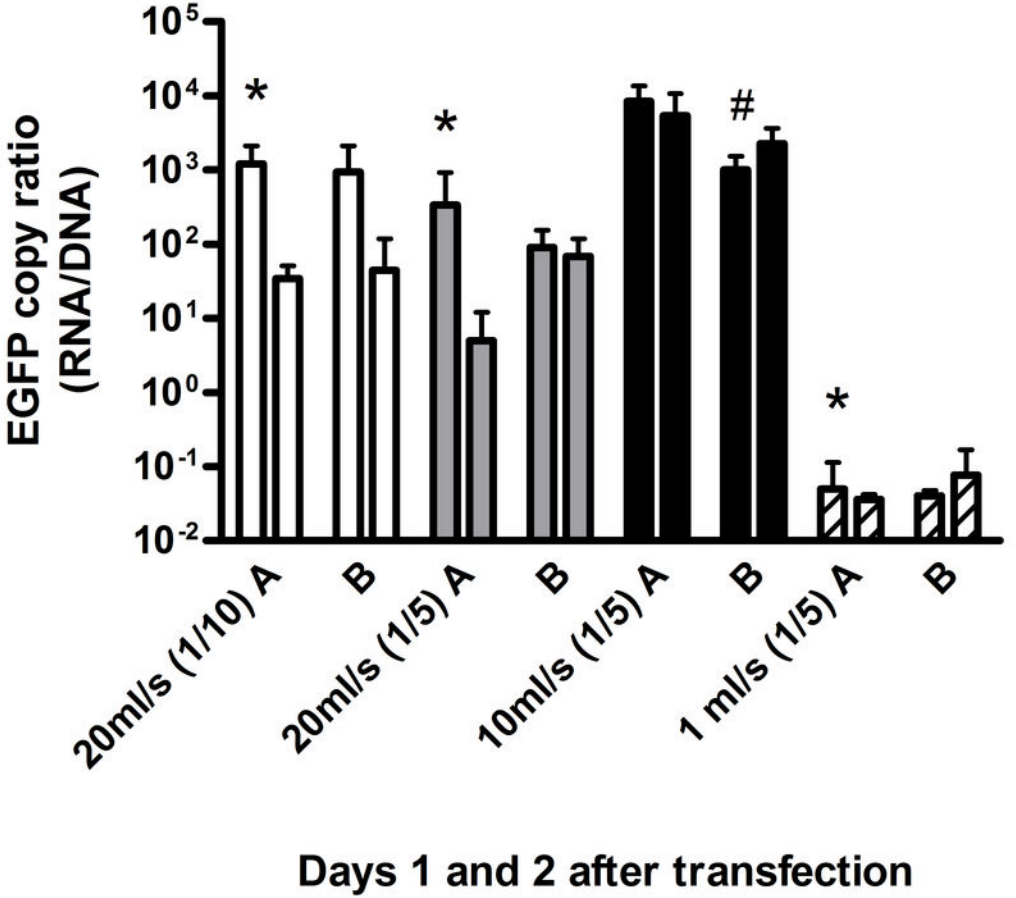

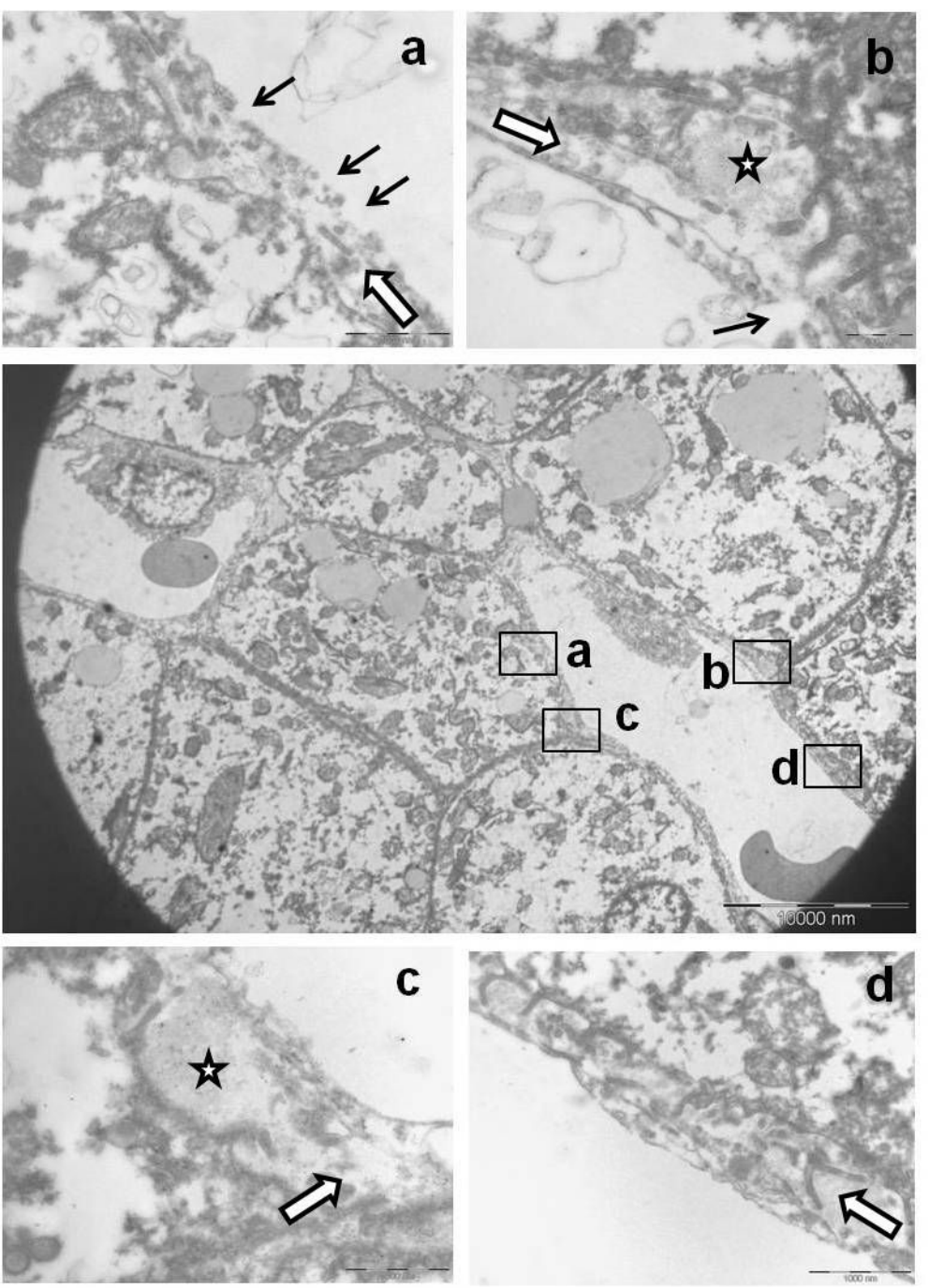
a
b
a
b
c
d
10000 nm
c
d

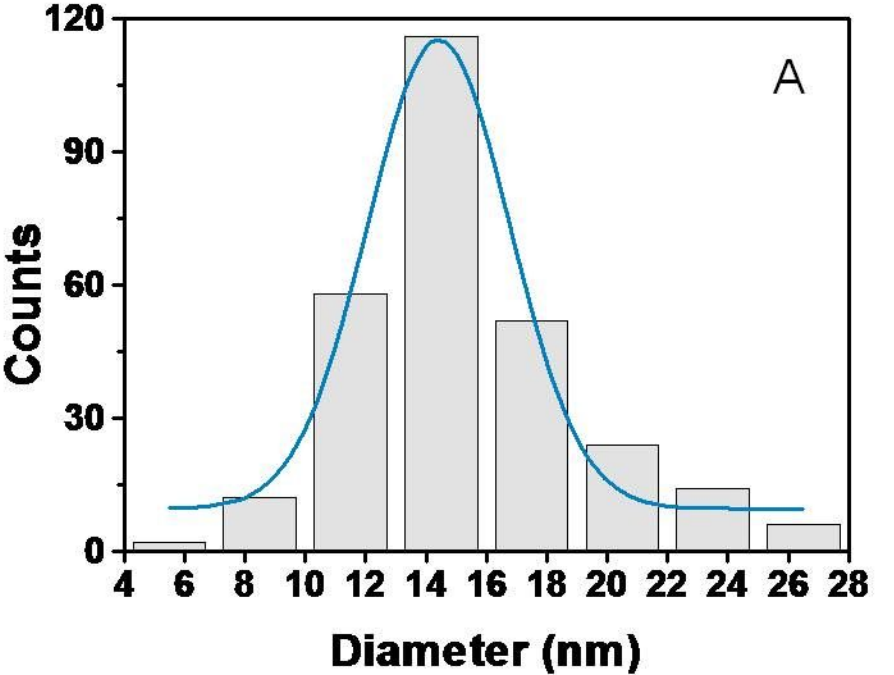
A
Counts
Diameter (nm)
0
30
60
90
120
4
6
8
10
12
14
16
18
20
22
24
26
28

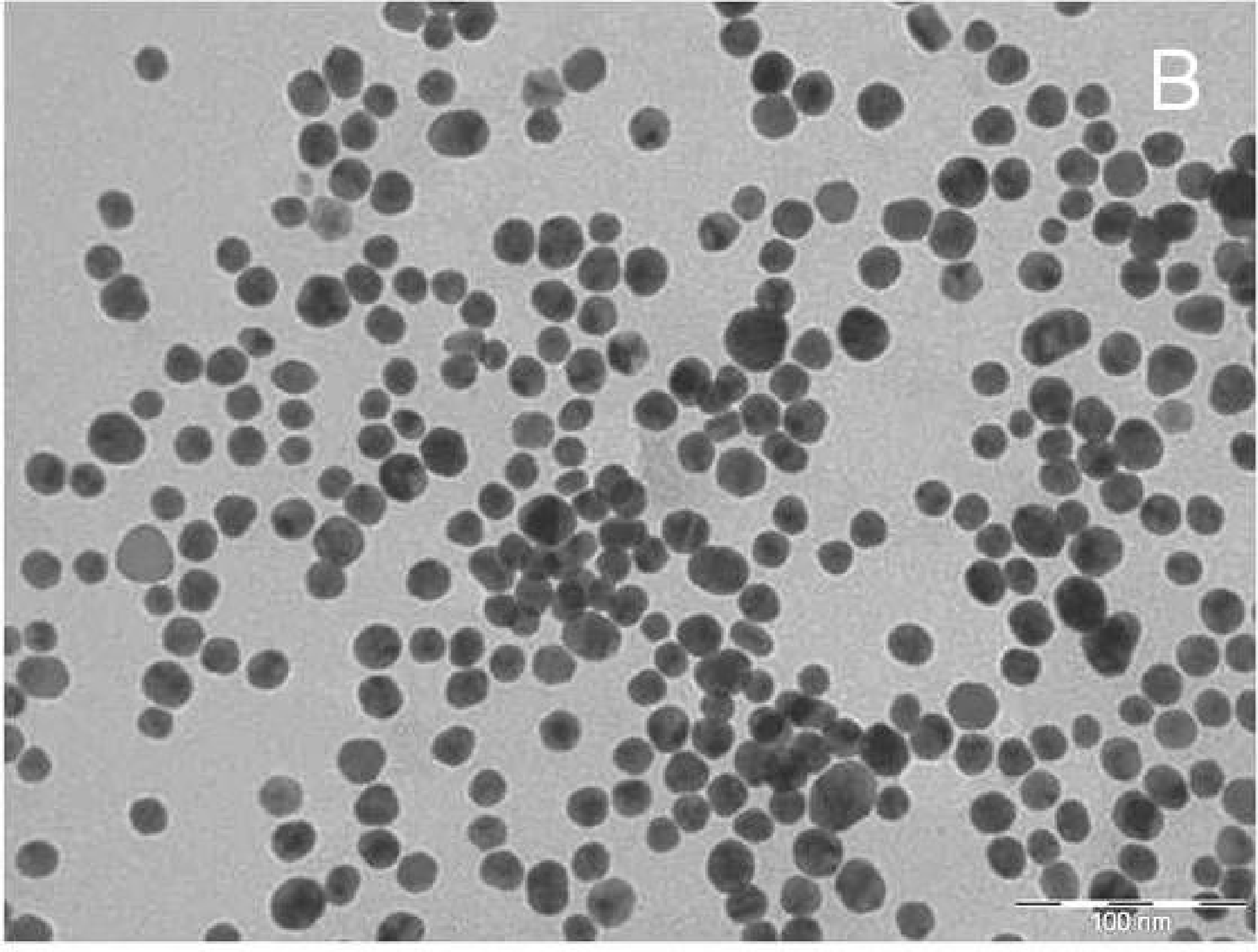

Au particles - TEM

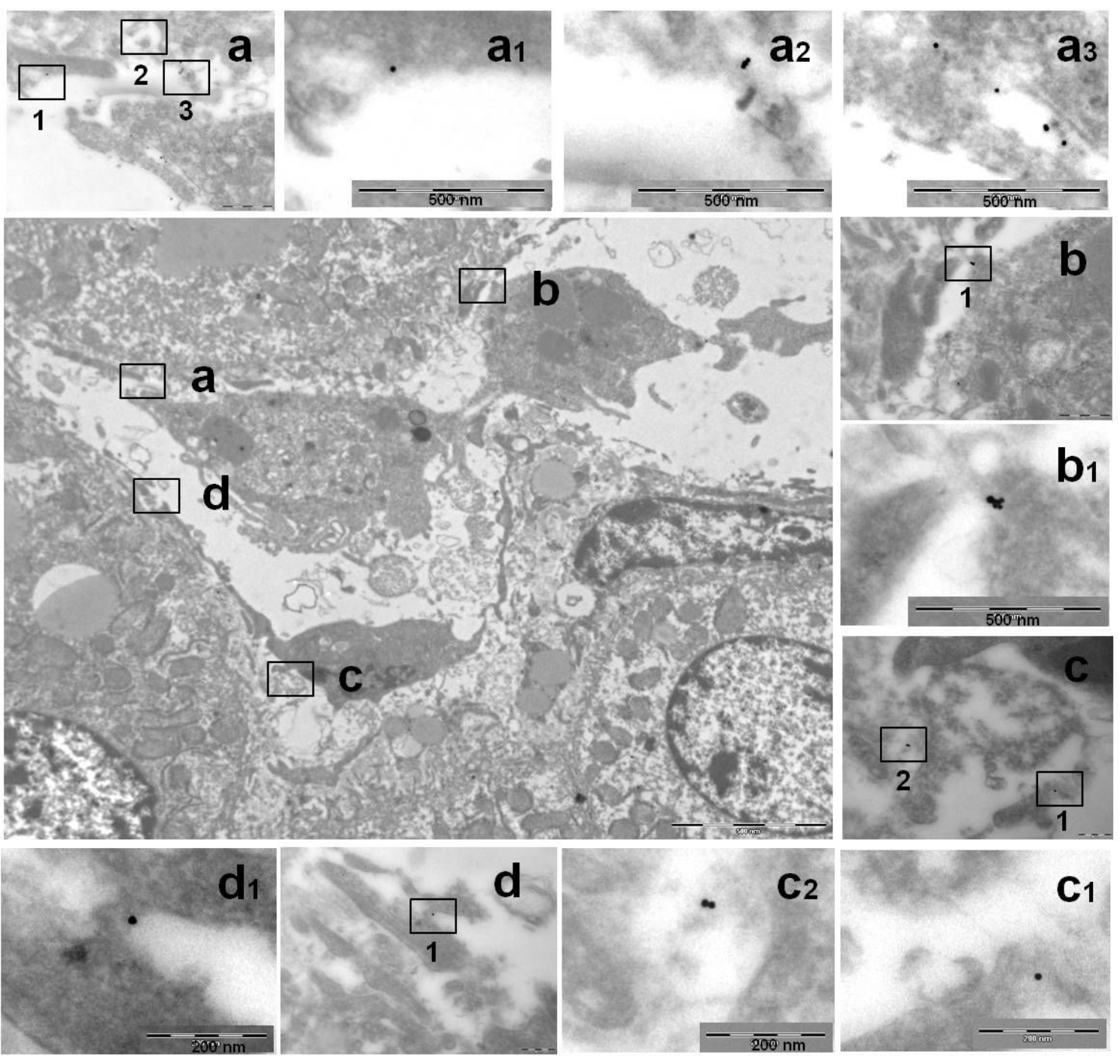
a
1
2
3
a1
500 nm
a2
500 nm
a3
500 nm
b
a
d
c
b
1
b1
500 nm
c
2
1
d1
200 nm
d
1
c2
200 nm
c1
200 nm

Table 1- Main characteristics of the human liver segments (HL) employed*. The table includes the experimental injection conditions performed and the kind of analyses in each segment, being PCR, molecular analyses of PCR and/or RT-PCR; F, optical fluorescence microscopy for eGFP protein; IHC, optical microscopy for immunohistochemistry of eGFP protein; TEM, transmission electron microscopy; TEM-Gold, transmission electron microscopy after gold nanoparticles injection.*

Experimental Conditions	**Experiment Number**	**Segment Localization**	**Segment Weight**	**Analyses Performed**
20ml/s, 1/10 n=5	HL01	VI and VII	500 g	PCR, F
	HL02	VI	404 g	PCR, F
	HL03	VII and VIII	450 g	PCR, F
	HL04	VIII	600 g	PCR
	HL05	II and III	446 g	PCR
20ml/s, 1/5 n=10	HL06	II and III	350 g	PCR
	HL07	II and III	157 g	PCR
	HL08	II and III	302 g	PCR
	HL09	V-VIII	815 g	PCR
	HL10	VII	200 g	TEM
	HL11	VI	310 g	TEM
	HL12	II and III	244 g	TEM
	HL13 HL14	VI II and III	294 g 440 g	TEM-Gold TEM-Gold
	HL15	II and III	290 g	TEM-Gold
10ml/s, 1/5 n=6	HL16	V-VIII	425 g	PCR
	HL17	VIII	110 g	PCR, IHC

	HL18	VI and VII	816 g	PCR,IHC
	HL19	II and III	312 g	PCR,IHC
	HL20	VI and VII	829 g	PCR
	HL21	V-VIII	987 g	PCR
1ml/s, 1/5 (“Control”) n=4	HL22	V	340 g	PCR, F, IHC
	HL23	VI and VII	342 g	PCR, F, IHC
	HL24	II and III	211 g	PCR, F, IHC
	HL25	II and III	277 g	PCR, F, IHC